Evaluation of Edge Configuration in Medical Echo Images Using Genetic Algorithms

Ching-Fen Jiang

Abstract—Edge detection is usually the first step in medical image processing. However, the difficulty increases when a conventional kernel-based edge detector is applied to ultrasonic images with a textural pattern and speckle noise. We designed an adaptive diffusion filter to remove speckle noise while preserving the initial edges detected by using a Sobel edge detector. We also propose a genetic algorithm for edge selection to form complete boundaries of the detected entities. We designed two fitness functions to evaluate whether a criterion with a complex edge configuration can render a better result than a simple criterion such as the strength of gradient. The edges obtained by using a complex fitness function are thicker and more fragmented than those obtained by using a simple fitness function, suggesting that a complex edge selecting scheme is not necessary for good edge detection in medical ultrasonic images; instead, a proper noise-smoothing filter is the key.

Keywords—edge detection, ultrasonic images, speckle noise

I. INTRODUCTION

CURRENTLY, there is increasing demand for clinical use of computer-aided diagnosis (CAD) in medical image analysis due to its advantages of repeatability and preciseness. It is usually performed through object extraction from an image for the assessment of the shape and size in two or even three dimensions. Low-level image processing tasks such as edge detection or segmentation are required to obtain a clear entity from the scenery. However, due to the low contrast and noisy nature of medical images, using conventional kernel-based edge detector alone does not usually yield satisfactory results for medical image tasks, especially for ultrasonic images.

Ultrasonic images are the most widely used diagnostic image due to their safety and relatively low cost. However, intrinsic drawbacks such as low contrast and the blurring of boundaries with speckle noise increase the difficulty in edge detection. Due to the speckle characteristics of echo images, many approaches to detect entities in them as regions with different textures from the background. These texture-based methods usually define various textural features and use these features to segment the objects such as the prostate [1-2], liver [3], and lung [4]. Segmentation can be accomplished a classifier such as neural networks [5] based on a set of textural features. We have successfully developed two types of classifiers to detect entities

in ultrasonic images: an unequal weighted k-means cluster [6] and a classifier based on genetic algorithms [7].

In contrast to region-based approaches mentioned above, a modified version of kernel-based edge detector has been proposed by Gudmundsson *et al.* [8] to detect edges in medical images. They used a genetic algorithm with a cost minimization process to refine the edge map from a medical image. Their edge map was defined as the dissimilarity in mean intensities between two adjacent regions. They claimed that their proposed algorithm is suitable for any medical images from different modalities. However, we found that it could not be successfully applied to ultrasonic images. After careful examination, we postulate that the failure may be due to their noise reduction process, where edges get blurred by the averaging process during the deviation of the edge map.

To address this problem, we developed a genetic algorithm with a modified noise reduction process that uses an anisotropic smoothing filter. We used several sets of ultrasonic images to evaluate the performance of this method for edge detection.

II. METHODS

A. Anisotropic smoothing filter

The concept for the anisotropic diffusion filter (ADF) was originally proposed by Perona and Malik to simulate image intensity averaging as a gas diffusion effect [9]. The difference of ADF from a general averaging filter is that a smoothing constraint makes the smoothing effect inconsistent at different directions. This constraint is a function of the intensity gradient, $g(\nabla I)$, which controls the soothing effect occurring in regions with homogeneous intensity while stopping at the edges. The overall process of the original ADF can be described as follows.

$$I_s^{t+1} = I_s^t + \frac{\lambda}{|\eta_s|} \sum_{p \in \eta_s} g(\nabla I_{s,p}^t) \nabla I_{s,p}^t \tag{1}$$

$$\nabla I_{s,p}^t = \nabla I_p^t - \nabla I_s^t , \ p \in \eta_s \tag{2}$$

where λ is a positive constant to control the diffusion rate; η_s is the neighbors of s; and $|\eta_s|$ is the number of pixels in η_s.

The essential idea of (1) is to iteratively adjust the intensity of the center pixel s in a square lattice by adding the mean of intensity differences between it and its neighbor pixels p in the

C. F. Jiang is an Associate Professor with the Department of Biomedical Engineering, I-Shou University, Taiwan (phone: 886-7-657-7711 ext. 6711; fax: 886-7-657-7711 ext. 6701; e-mail: cfjiang@-isu.edu.tw).

lattice. As the iteration number t increases, the resolution of the corresponding processing image becomes coarser. The original lattice structure in Perona and Malik's approach was 3×3 and only contained the neighbor pixels p in the vertical and horizontal directions. Their smoothing control function $g(\nabla I)$ was a sigmoidal function, which indicates the value of $g(\nabla I)$ getting smaller as ∇I increases and therefore leads to a less smooth effect. Their study showed that ADF performed well for three images with good region homogeneity. However, when considering the edge detection from images with noise distribution, the design of $g(\nabla I)$ becomes a crucial task for removing the noise but preserving the edges.

For adaptation to medical images tasks, such as removing patch-style noises and preserving ramp edges, we have previously proposed a modified adaptive diffusion filter [10] based on the ADF algorithm. The lattice size was enlarged to 5. In addition, we defined the smoothing control function $g(x)$ as the function of the *local regional difference* instead of the intensity gradient as in (3).

$$g(x) = \exp\left(\frac{- SD_{i,j} \cdot x^2}{ak}\right), x \in \{\nabla V_s, \nabla H_s, \nabla L_s, \nabla R_s\} \qquad (3)$$

where ∇V_s, ∇H_s, ∇L_s, and ∇R_s denote the intensity differences between regions in the *vertical*, *horizontal*, *right diagonal*, and *left diagonal* directions, respectively. $SD_{i,j}$ is defined as in (4).

$$SD_{i,j} = \sqrt{\tfrac{1}{25} \sum_{x=-2}^{2} \sum_{y=-2}^{2} (I_{i+x,j+x} - M_{i,j})^2} \qquad (4)$$

where (i, j) is the coordinate of the central pixel s. $M_{x,y}$ is the intensity mean of the 5×5 lattice centered at (x, y).

The scale factor of $SD_{i,j}$ in $g(x)$ can improve the smoothing performance, i.e., the homogeneous regions become smoother and more integrated; meanwhile, the edges keep unchanged.

B. Genetic Algorithms

After applying anisotropic diffusion, a gradient map was derived by convolving the smoothed image with a Sobel mask [11]. The genetic algorithm was developed to select the surviving gradients on the gradient map to form the final boundaries.

The overall procedure of the genetic algorithms is depicted as in Fig. 1.

```
Input gradient map
For (for every pixel i)
   { Do (select fitness function- fitnessi)
      {calculate fitnessi
         Call (Genetic algorithm) }
      Output the edge configuration}
EndDo
```

```
Do (Genetic algorithm)
   while ([ (fitness(max) - fitness(min)) / (sum of fitnessi) ] < 0.1)
{ Crossover(gradient imagei)
   Mutation(gradient imagei)
   Reproduction }
      EndDo
   EndLoop
```

Fig. 1 Pseudo code of the genetic algorithm

We defined two fitness functions. One is simply defined as the strength of the gradient $g(\cdot)$ as in (5). The other is the reciprocal of the cost function C, which is the summation of each feature cost as in (6)

$$fitness_1 = g(\cdot) \qquad (5)$$

$$fitness_2 = \frac{1}{C} = \frac{1}{(C_d + C_f + C_m + C_c)} \qquad (6)$$

where C_d is the cost of a gradient, C_f is the cost of fragments, C_m is the cost of connectivity, and C_c is the cost of curvature. These are defined as

$$C_f(S) = \begin{cases} 1.0, \text{ if s is an isolated end point} \\ 0.5, \text{ if s is a nonisolated end point} \\ 0, \quad \text{otherwise} \end{cases} \qquad (7)$$

$$C_d = \begin{cases} 1 \quad\quad, \text{if } g(\cdot) = 0 \\ 1/g(\cdot) \text{ ,otherwise} \end{cases} \qquad (8)$$

$$C_m = \begin{cases} 0.5 \text{ or } 1, \text{if } n \geq 3 \\ 0 \text{ or } 1, \text{if } n = 2 \\ 0.5, \text{if } n = 1 \\ 1, \text{if } n = 0 \end{cases} \qquad (9)$$

where n is the number of connected pixels. When n equals 2 and the connection fits one of the two-connective patterns in Fig. 2, then C_m is set to 0; otherwise, it is set to 1. When n equals 3 and the connection fits one of the three-connective patterns in Fig. 3, then C_m is set to 0.5; otherwise, it is set to 1.

$$C_c(S) = \begin{cases} 0, \text{ if } \theta = 0 \\ 0.5, \text{ if } \theta = 45 \\ 1.0, \text{ if } \theta \geq 90 \end{cases} \qquad (10)$$

where θ is the angle between two edges.
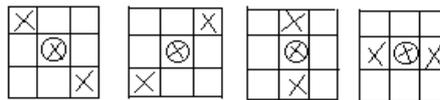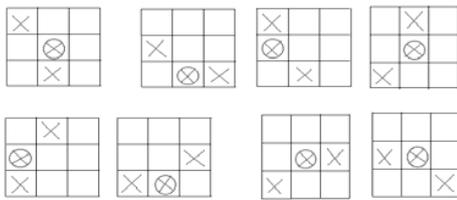
Fig. 2 Two-connective patterns for efficient edges points
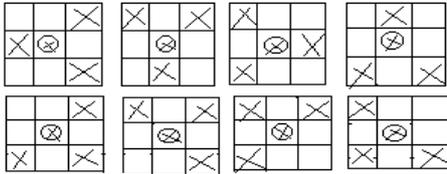
Fig. 3 Three-connective patterns for efficient edges points

The determination of the total cost through summation of each feature cost can be summarized through a decision tree, as shown in Fig. 4.
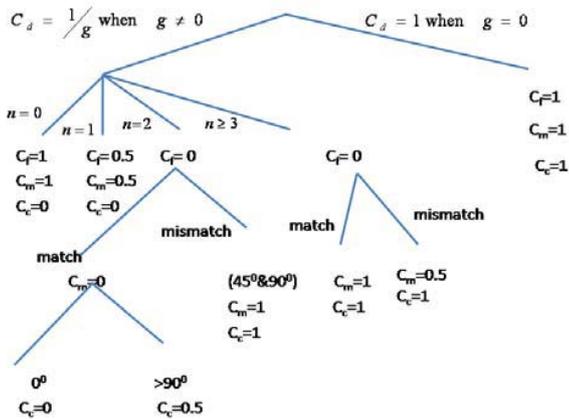
Fig. 4 Decision tree to determine the value of each feature cost along the path

A good edge structure can be obtained by minimizing the cost function; therefore, we adopted it to calculate the fitness for deciding whether the edge will be preserved for next generation. The GA stops when the predefined condition (indicated as the while-condition in the second Do-loop in Fig. 2) is met.

Crossover is carried out by randomly selecting one pair of chromosomes encoded as binary values of x and y coordinates to exchange their y-coordinates, as shown in Fig.5. Mutation of a chromosome is accomplished by converting the y-coordinate to its compliment. The evolution parameters were set empirically as shown in Table I. The best genes, i.e., the best edge in the gradient map, survive after crossover and mutation for several generations.
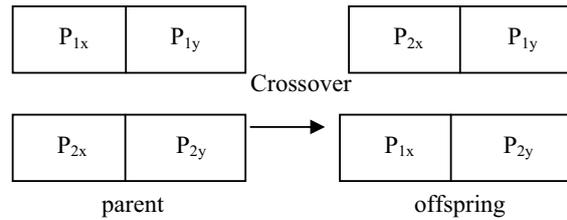
Fig. 5 Crossover process

TABLE I
EVOLUTION PARAMETERS

GA Type	Crossover Rate, P_C	Mutation Rate, P_M
GA with fitness$_1$	0.1	0.01
GA with fitness$_2$	0.08	0.01

III. RESULTS

Two examples are given in this section to illustrate the results for each processing stage. The original images were acquired by using a KV 530D 3-D ultrasound machine from the Department of Gynecology, National Cheng-Kung University Hospital. Fig 6 shows the noise-removing effect of the proposed adaptive diffusion filter. In comparison to the original ovarian image in Fig. 6a, Fig. 6b demonstrates that the filter can remove the speckle noises and preserve integrated regions without smearing the boundaries. The final edge configurations selected by the genetic algorithm with fitness$_1$, as in (5), and fitness$_2$, as in (6), are shown in Figs. 6c and 6d, respectively. The boundaries in Fig. 6d are thicker but more sparsely distributed than those shown in Fig. 6c.

(a)   (b)

(c)   (d)
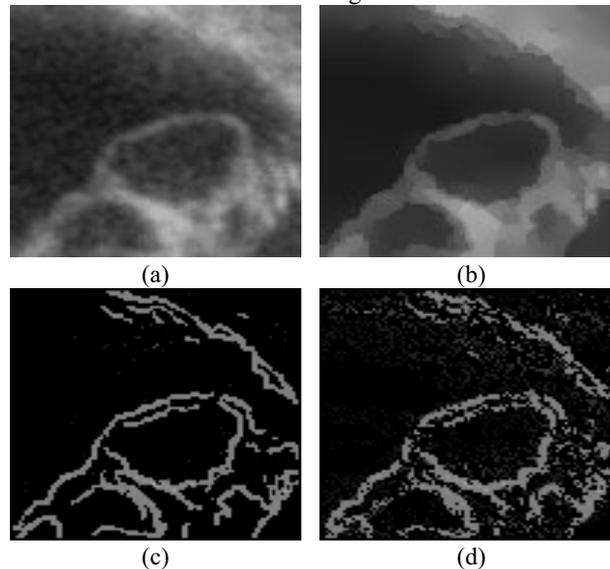
Fig. 6 Ovarian ultrasonic image. (a) Original image, (b) noise-removed image through the proposed anisotropic diffusion filter, (c) final edge configuration by using fitness$_1$, and (d) final edge configuration by using fitness$_2$.

(a)   (b)

(c)   (d)
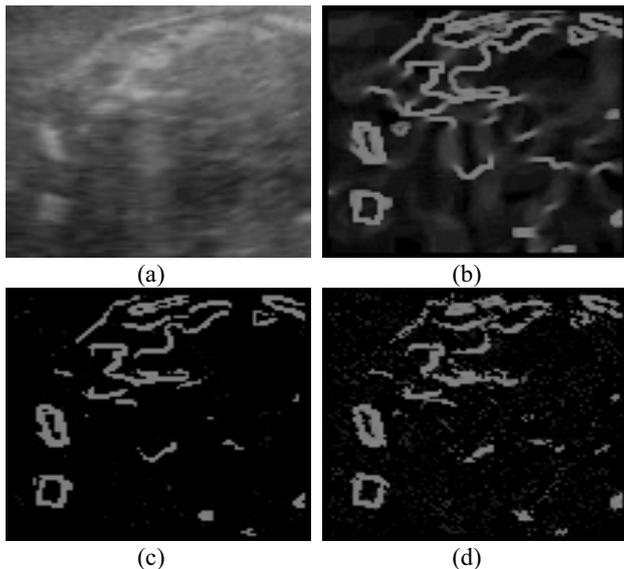
Fig. 7 Ultrasonic image of a fetal spine. (a) Original image, (b) gradient map detected from the noise-removed image by using the Sobel filter, (c) final edge configuration by using fitness$_1$, and (d) final edge configuration by using fitness$_2$.

Fig. 7 shows the comparison of edge configurations before and after the GA process. In comparison with the gradient map (Fig. 7b) detected from the noise-removed image by using the Sobel filter, both edge configurations selected either by using fitness$_1$ (Fig. 7c) or fitness$_2$ (Fig. 7d) reduced a certain amount of redundant edges. However, Fig. 7d still presents a thinner and more compact edge structure than that shown in Fig. 7c.

IV. DISCUSSION

Ultrasonic images are the most widely used diagnostic image in various clinics. However, its textural pattern with speckle noise decreases the differentiability between different entities, which increases the difficulty in object recognition. In image processing tasks for assisting in object detection in such images, speckle noise removal is usually the first step to enhance the integrity of different regions. Once the speckle noise is reduced, the boundary of the body can be more integrated for later detection.

Due to the complexity of anatomical structures contained in medical images, special attention should be paid to the design of the edge detector for medical images. A genetic algorithm developed by Gudmundsson *et al.* is aimed at detecting an optimal edge configuration that meets several constraints defined by feature costs. The optimal edge configuration was extracted through GA from the initial edge map, which was derived by using a conventional edge detector associated with the averaging filter. They demonstrated satisfactory results for T1-weighted MR images. However, our pilot study on applying this scheme to ultrasonic images was not successful. We postulate that the averaging process for noise removal may have induced this failure. The most commonly used smoothing

filters such as averaging and median filters reduce noise by decreasing the intensity gradients into a certain range on the basis of the intensity similarity of a pixel with that of its neighbors. However, both of these filters are not suitable for smoothing medical images with low contrast and unclear edges with the interference of patch-style noise, such as ultrasound. Unlike white noise, this type of noise cannot be removed by using a point-based filter; instead, it needs to be addressed and treated regionally.

We therefore developed an adaptive diffusion filter to replace the averaging filter used for noise removal. We also proposed two fitness functions for the GA scheme to evaluate whether a complex edge selection scheme can render a better result than a simple criterion such as the strength of the gradient. The edges obtained by using a complex fitness function were thicker and more fragmented than those obtained by using a simple fitness function, suggesting that a complex edge selecting scheme is not necessary for good edge detection in medical ultrasonic images; instead, a proper noise-smoothing filter is the key.

REFERENCES

[1] Y. Q. Zhan and D. G. Shen, "Deformable segmentation of 3-D ultrasound prostate images using statistical texture matching method," *IEEE Trans. on Medical Imaging,* vol. 25, pp. 256-272, Mar 2006.
[2] W. D. Richard and C. G. Keen, "Automated texture-based segmentation of ultrasound images of the prostate," *Comput Med Imaging Graph,* vol. 20, pp. 131-40, May-Jun 1996.
[3] C. M. Wu, and Y. C. Chen, "Texture feature for classification of ultrasonic liver images", *IEEE Trans. Med. Imaging*, vol. 11, pp. 141-152, 1992.
[4] K. N. Bhanu Prakash*, et al.*, "Fetal lung maturity analysis using ultrasound image features," *IEEE Trans.on Information Technology in Biomedicine,* vol. 6, pp. 38-45, 2002.
[5] S. Pavlopoulos, and et. al. –"Fuzzy neural Network-Based Texture Analysis of Ultrasonic Images", –*IEEE Engineering in Medicine and Biology*, -vol.19, no. 1, pp39-47, 2000
[6] C.F. Jiang, "3D image reconstruction of ovarian tumor in the ultrasonic images, *Biomedical Engineering-Applications, Basis & Communications"*, vol. 13; pp 41-46, 2001.
[7] Y. C. Hsu, C.F. Jiang, and C. M. Uang, "Auto-segmentation of ultrasonic images by the genetic algorithm", *Journal of Medical and Biological Engineering*, vol. 21, no.2 ,pp. 121-126, 2001.
[8] M. Gudmundsson, E.A. El-Kwae, and M.R. Kabuka, "Edge detection in medical images using a genetic algorithm," *IEEE Trans. Medical Imaging*, **17**, pp. 469-474, 1998
[9] P. Perona, and J. Malik, "Scale-space and edge detection using anisotropic diffusion," *IEEE Trans. Patt. Anal. Mech. Intell.*, PAMI-12, no. 7, pp. 629-639, 1990
[10] S.R. Wang, Y.N. Sun, F.M. Chang, and C. F. Jiang, "3D image display of fetal ultrasonic image by thin shell," *SPIE on Medical Imaging*, pp.1478-1488, San Diego, USA, 1999.
[11] R.C. Gonzalez and R.E. Woods, *Digital Image Processing*, Addison-Wesley, 2002, Ch. 10.